



## Research Paper

---

Author should please send Table 2 and provide year to the references colored red in the work.

# The cosmological effect of CMB/BAO measurements

Accepted date

## ABSTRACT

Yi Zhang<sup>1,2</sup>

<sup>1</sup>College of Science, Chongqing  
University of Posts and  
Telecommunications,  
Chongqing 400065, China.

<sup>2</sup>State Key Laboratory of  
Theoretical Physics, Institute of  
Theoretical Physics, Chinese  
Academy of Science,  
Beijing 100190, China.

E-mail: zhangvia@caupt.edu.cn.

In this paper, the CMB/BAO measurements which cover the 13 redshift data in the regime  $0.106 \leq z \leq 2.34$  are given out. The CMB/BAO samples are based on the BAO distance ratios  $r_s(z_d)/D_V(z)$  and the CMB acoustic scales  $l_A$ . It could give out the accelerating behaviors of the  $\Lambda$ CDM,  $w$ CDM and  $\phi$ CDM models. As the direction of the degeneracy of  $\Omega_{m0} - w$  and  $\Omega_{m0} - \Omega_{k0}$  are different for the CMB/BAO and BAO data, the CMB/BAO data show ability of breaking parameter degeneracy. We observed constraining results from the BAO+Planck/BAO+ $\Omega_b h^2 + \Omega_m h^2$  data which has  $\Omega_{m0}$  tension but does not have  $H_0$  tension with the Planck result. The extending parameters  $w$  and  $\Omega_{k0}$  could alleviate the  $\Omega_{m0}$  tensions slightly.

**Key words:** CMB/BAO measurements, cosmological effect.

## INTRODUCTION

The CMB/BAO data (Sollerman, 2009) is a kind of observational data which try to exact more information from the important cosmological experiments: CMB (Cosmic Microwave Background) and BAO (Baryon Acoustic Oscillation). The CMB probes the rate of the expansion at redshift  $z \sim 1100$  (Bennett, 2013; Ade, year) and the BAO technique provides a distance-redshift relation at low redshifts (Percival et al., 2007; Beutler, 2011; Percival, 2010; Kazin, 2010; Padmanabhan et al., 2012; Blake, 2011; Anderson, year; Delubac, year; Blake, 2011; Anderson et al., 2013; Busca et al., 2013). CMB and BAO are observations to different issues and challenges, and is affected by different physics; one is by any non-standard early-universe physics, while the other is by late time expansion mainly. Typically, the CMB/BAO cosmological constraining results are discussed with other low-redshift data or the CMB data to fix tightly constraining portions of parameter space. In this letter, the CMB/BAO data is sufficient to permit a meaningful comparison with type IA supernovae (SNe) measurement without strong CMB priors.

In the first CMB/BAO paper (Sollerman, 2009) the number of CMB/BAO data is just 2. As BAO survey<sup>1</sup> develops the number is increased to 5 (Bennett, 2013; Busca et al., 2013; Veropalumbo et al., year). To make clear the constraining effects of the CMB/BAO data, 13 observational BAO data were collected and the Planck or WMAP9 survey selected. One benefit of the BAO data is that it is limited by the statistical error, rather than systematic uncertainties (Li et al., 2013). As the newly released CMB data, Planck results consist of results from BAOs data (Lazkoz et al., 2013). We concentrated on testing the  $\Lambda$ CDM model and its extensions with the CMB/BAO data.

The rationale for considering the  $\Lambda$ CDM model is that one could consider the cosmo- logical constant as a “null

---

<sup>1</sup>In the simulated BAO data which has 21 data (Manera et al., 2012) the  $\Lambda$ CDM model could be constrained as well.

**Table 1:** The BAO and CMB/BAO samples are derived from 6dFGS, SDSS LRG, WiggleZ, BOSS DR11, Planck and WAMP9.

Redshift $z$	$r_s(z_d)/D_V(z)$	$f(\text{Planck}/\text{BAO})$	$f(\text{WMAP9}/\text{BAO})$	$f(\text{WMAP9}(w)/\text{BAO})$	BAO
0.106	$0.336 \pm 0.015$	$31.56 \pm 1.44$	$30.82 \pm 1.43$	$30.85 \pm 1.43$	(Beutler, 2011) 6dFGS
0.20	$0.1905 \pm 0.0061$	$17.95 \pm 0.60$	$17.53 \pm 0.60$	$17.54 \pm 0.60$	
0.35	$0.1097 \pm 0.0036$	$10.33 \pm 0.35$	$10.09 \pm 0.35$	$10.10 \pm 0.35$	(Percival, 2010) SDSS LRG
0.275	$0.1390 \pm 0.0037$	$13.09 \pm 0.37$	$12.79 \pm 0.37$	$12.80 \pm 0.37$	
0.278	$0.1389 \pm 0.0043$	$13.08 \pm 0.42$	$12.78 \pm 0.42$	$12.79 \pm 0.42$	(Kazin, 2010) SDSS LRG
0.35	$0.1126 \pm 0.0022$	$10.61 \pm 0.23$	$10.36 \pm 0.24$	$10.37 \pm 0.24$	(Padmanabhan, 2012) SDSS LRG
0.314	$0.1239 \pm 0.0033$	$11.67 \pm 0.33$	$11.40 \pm 0.33$	$11.41 \pm 0.33$	
0.44	$0.0916 \pm 0.0071$	$8.63 \pm 0.67$	$8.43 \pm 0.66$	$8.44 \pm 0.66$	(Blake, 2011) SDSS LRG
0.60	$0.0726 \pm 0.0034$	$6.84 \pm 0.33$	$6.68 \pm 0.32$	$6.69 \pm 0.32$	
0.73	$0.0592 \pm 0.0032$	$5.58 \pm 0.31$	$5.45 \pm 0.30$	$5.45 \pm 0.30$	
0.32	$0.1212 \pm 0.0024$	$11.42 \pm 0.25$	$11.15 \pm 0.26$	$11.16 \pm 0.26$	(Anderson, year) BOSS DR11
0.57	$0.0732 \pm 0.0012$	$6.90 \pm 0.13$	$6.73 \pm 0.14$	$6.74 \pm 0.14$	
2.34	$0.0320 \pm 0.0007$	$3.01 \pm 0.07$	$2.94 \pm 0.07$	$2.95 \pm 0.07$	(Delubac, year) BOSS DR11

hypothesis" for dark energy, so it is worth exploring if it provides a reasonable description of data. As our dataset becomes larger, whether the dataset is suitable to standard  $\Lambda$ CDM model is an interesting question. A hypothetical deviation from  $\Lambda$ -acceleration may first appear as a tension between CMB and low-redshift data, or arise from statistical fluctuations and systematic uncertainties that are incorrectly correctly quantified, alternatively extensions to the standard model, or some combinations of these factors. The ability to disambiguate these possibilities from current and future low-redshift experiments is crucial. Therefore, we considered  $w$ CDM which adopted a constant  $w$  (the equation of state of dark energy  $p_d/\rho_d$ ) and  $o\Lambda$ CDM model which extends this model to non-zero dimensionless energy density of curvature  $\Omega_k$  as well.

In this paper, we use improved CMB/BAO data to constrain the  $\Lambda$ CDM,  $w$ CDM and  $\Lambda$ CDM models.

## METHODOLOGY

The acoustic peak in the galaxy correlation function provides a standard ruler  $r_s(z_d)/D_V(z)$  (or its inverse  $D_V(z)/r_s(z_d)$ ) which measure the distance to objects at redshift  $z$  of recombination in unit of the sound horizon. The sound horizon and the dubbed spherically averaged distance are:

$$r_s(z_d) = \int_{z_d}^{\infty} \frac{c_s(z) dz}{H(z)},$$

$$D_V(z) = \left( \frac{(1+z)^2 d_A(z_*)^2 c_{\beta}}{H} \right)^{1/3},$$

Where  $H$  is the Hubble parameter,  $c_s$  is the speed of sound

before recombination,  $d_A(z_*)$  is the co-moving angular diameter distance to recombination,  $z_*$  is the redshift at recombination with the value of 1090.48 and  $z_d$  is the value of the redshift of the drag epoch which is gotten by the fitting formula (Zhang et al., 2013).

The observable quantities of BAO are only sensitive to the early universe physics through the sound horizon  $r_s(z_d)$ , while the CMB data provide an excellent standard ruler as well which is the position of the first CMB power spectrum peak which represents the angular scale of sound horizon at recombination  $z_*$  and the dubbed acoustic scale:

$$l_A = \frac{\pi d_A(z_*)(1+z_*)}{r_s(z_*)}$$

The CMB/BAO parameter  $f$  is regarded to be more suitable than the primitive CMB shift parameter  $l_A$  for non-standard dark energy model (Sollerman, 2009; Busca et al., 2013; Veropalumbo et al., year):

$$f(z) = \frac{l_A}{\pi} * \frac{r_s}{D_V(z)} * \frac{r_s(z_*)}{r_s(z_d)} = \frac{d_A(z_*)}{D_V(z)},$$

$$\frac{\sigma_f}{f} = \sqrt{\left(\frac{\sigma_{l_A}}{l_A}\right)^2 + \left(\frac{\sigma_{BAO}}{r_s(z_*)/D_V(z)}\right)^2 + \left(\frac{\sigma_{r_s(z_d)/r_s(z_*)}}{r_s(z_d)/r_s(z_*)}\right)^2},$$

Where  $\sigma$  presents the error bar and  $f$  is regarded to have the ability of removing the dependence on much of the complex pre-recombination physics which is needed to determine the horizon scale. We further introduced the BAO and CMB samples separately.

## The BAO distance ratio

We list the BAO data  $r_s(z_d)/D_V(z)$  in Table 1 which are

derived from the 6dF Galaxy Redshift Survey (6dFGS), Sloan Digital Sky Survey Luminous Red Galaxy sample ((SDSS LRG), WiggleZ, Baryon Oscillation Spectroscopic Survey (BOSS) DR11 surveys<sup>2</sup>. The  $r_s(z_d)/DV(z)$  data was detected over a range of redshifts from  $z = 0.106$  to  $z = 2.34$  given as:

- 1) Beutler (2011) analyzed the large-scale correlation function of the 6dFGS and made a 4.5% measurement at  $z = 0.106$ ;
- 2) Percival (2010) measured the distance ratio  $dz = r_s(z_d)/DV(z)$  at redshifts  $z = 0.2$ , and  $z = 0.35$  by fitting to the power spectra of luminous red galaxies and main-sample galaxies in the SDSS. They also showed how the distance-redshift constraints at those two redshifts could be decomposed into a single distance constant at  $z = 0.275$  and a “gradient” around this pivot given by  $DV(0.35)/DV(0.2)$ . Furthermore, Kazin (2010) examined the correlation function  $\xi$  of the SDSS LRG at large scales using the final data release and get the BAO data at  $z = 0.278$ . Furthermore, Padmanabhan et al. (2012) applied the reconstruction technique to the clustering of galaxies from the SDSS LRG sample, sharpening the BAO feature and achieving the BAO result for  $z = 0.35$ ;
- 3) Blake et al. (2011) gave out the BAO feature in three bins centered at redshifts  $z = 0.44$ ,  $0.60$ , and  $0.73$  respectively, using the full sample of 158741 galaxies from WiggleZ survey. They also presented a new measurement of the baryon acoustic feature in the correlation function of the SDSS LRG sample and derived a BAO measurement at  $z = 0.314$  that is consistent with previous analyses of the LRG power spectrum;
- 4) Fitting for the position of the acoustic features in the correlation function and matter power spectrum of BAO in the clustering of galaxies from BOSS DR 11, Anderson et al. (2013) got the BAO result for  $z = 0.32$  and  $z = 0.57$  (Kazin, 2010). From BOSS DR11 latest released sample, Delubac (year) figured out the BAO feature in the flux-correction function of the Lyman- $\alpha$  forest of high redshift quasars at the effective redshift  $z = 2.34$  (Padmanabhan et al., 2012).

## The acoustic scale

The CMB anisotropies have been measured with ever increasing precision by missions such as WMAP9 (Bennett, 2013), Planck (Ade, year) and BICEP2 (Addison et al., 2013). The declaration that detects the CMB B-mode polarization by the BICEP2 collaboration Addison et al., 2013) might be wholly or partly due to polarized dust

<sup>2</sup>Our BAO data only use the distance ratio, not the other BAO parameter, e.g. the acoustic parameter. Thus, our BAO-only constraining results is different from the result of Lazkoz et al. (2013), Weinberg et al. (2013) Eisenstein and Hu (1997).

emission (Aubourg et al., year). For conciseness, we chose the Planck and WMAP9 data only. Indeed, the  $l_A$  parameter depends slightly on the background model (Wang et al., 2012).

The used acoustic scale  $l_A(z_*)$  and  $r_s(z_d)/r_s(z_*)$  at the decoupling redshift derived by Cheng and Huang, (year) and Ade (2014) is given as:

$$\text{Planck} + \text{lensing} + \text{WP}: l_A = 301.57 \pm 0.18(0.06\%) \left[ \frac{r_s(z_d)}{r_s(z_*)} = 1.019 \pm 0.009(0.88\%) \right]$$

$$\text{WMAP9}: l_A = 302.02 \pm 0.66(0.22\%), \frac{r_s(z_d)}{r_s(z_*)} = 1.045 \pm 0.012(1.15\%),$$

$$\text{WMAP9}(w): l_A = 302.35 \pm 0.65(0.21\%), \frac{r_s(z_d)}{r_s(z_*)} = 1.045 \pm 0.012(1.15\%).$$

The First CMB data combined with Planck lensing, as well as, WMAP polarization at low multipoles ( $l \leq 23$ ) (Ade, year) which represents the tightest constraints from CMB data only at present. The second one is derived from the  $\Lambda$ CDM model (Cheng and Huang, year; Ade, 2014) and WMAP9 data. The third one is derived from the  $w$ CDM model and WMAP9 data (Bennett, 2013). To distinguish the three kinds of CMB/BAO data, we call them Planck/BAO, WMAP9/BAO, and WMAP9( $w$ )/BAO separately. As Cai et al. (year) shows the  $l_A$  values vary if the fitting model is changed. Our results show that the value of  $l_A$  nearly does not affect the constraining results.

Based on BAO and CMB data, our CMB/BAO sample has 13 data which are presented in Table 1. The WMAP9( $w$ )/BAO data covers a total 5 CMB/BAO (Busca et al., 2013). Comparing the error in the BAO data, the CMB data will bring less uncertainty than BAO to the CMB/BAO, but the entire CMB/BAO data uncertainty has larger error than the BAO data. Our results show a tighter constraint from the CMB/BAO data as compared with BAO data (Table 2).

## The theoretical models

This accelerating behavior of our universe is usually attributed by a presently unknown component, called dark energy, which exhibits negative pressure and dominates over the matter-energy content of our universe. So far, the simplest candidate for dark energy is the cosmological constant, while the so-called standard cosmological model  $\Lambda$ CDM is in accordance with almost all the existing cosmological observations. As the CMB/BAO method retains sensitivity to phenomena that have more effect at higher redshift, such as curvature, we extend the constraining model to  $w$ CDM (the standard cosmological model with constant dark energy equation of state) and  $\Lambda$ CDM (the standard cosmological model with curvature). It means we use the following parameters: the equation of state of dark energy  $w$ , Hubble parameter  $H$ , and the dimensionless energy density parameter for the matter  $\Omega_{m0}$  and the curvature  $\Omega_{k0}$ .

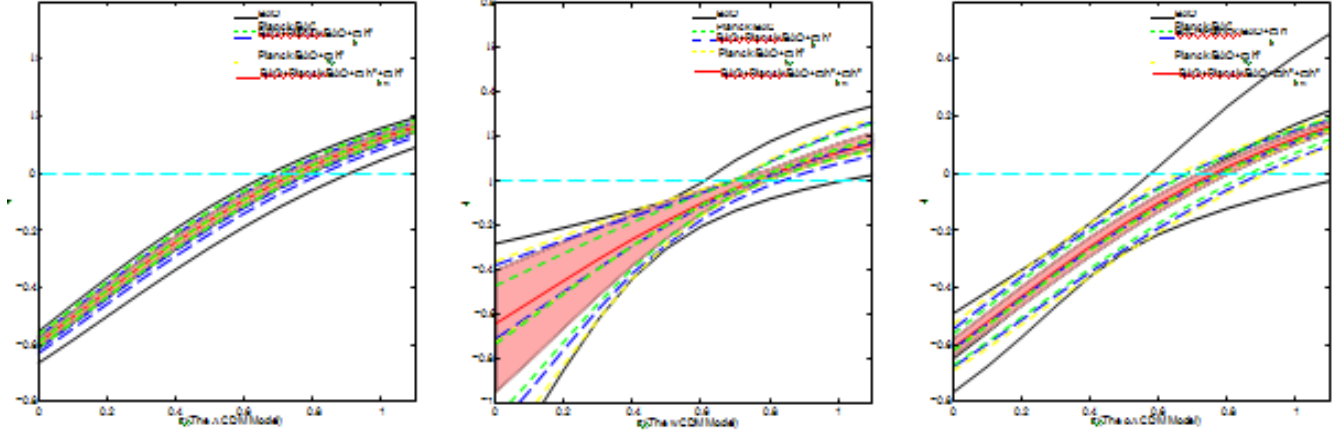


**Figure 1:** The evolution of the deceleration parameter  $q$  vs the redshift  $z$  for selected data.

The BAO position measurements do not provide any  $H_0$  constraint, being sensitive only to the combination  $H_0 r_s$ . The sound horizon depends on the physical baryon density,  $\Omega_b h^2$ , through  $r_s \propto (\Omega_b h^2)^{-0.13}$ . We then add the prior  $\Omega_b h^2 = 0.0223 \pm 0.0009$  (Pettini and Cooke, 2012) to the BAO data by fixing the CMB mean temperature, which is fixed to 2.73 K and determines the energy density in radiation. On the other hand, the CMB/BAO data is independent from the sound horizon, thus, CMB/BAO-only data could not constrain  $H_0$ . Correspondingly, we add the  $\Omega_m h^2 = 0.1199 \pm 0.0027$  prior from Planck to the CMB/BAO for the  $H_0$  constraint.

For data comparison convenience, we divide the data into three samples: (1) the CMB related data Planck/BAO (or  $+\Omega_m h^2$ ), WMAP/BAO (or  $+\Omega_m h^2$ ), WMAP(w)/BAO (or  $+\Omega_m h^2$ ); (2) the BAO data related data: BAO (or  $+\Omega_b h^2$ ), BAO+Planck/BAO (or  $+\Omega_b h^2$ ), BAO+WMAP/BAO (or  $+\Omega_b h^2$ ); (3) all combined data: BAO+Planck/BAO  $+\Omega_b h^2 + \Omega_m h^2$ , BAO+WMAP/BAO  $+\Omega_b h^2 + \Omega_m h^2$ . Thereafter, we used the Monte Carlo Markov Chain (MCMC) method based on the publicly available package COSMOMC (Lewis and Bridle, 2002) to constrain model parameters which randomly chooses values for the aforementioned parameters, evaluates  $\chi^2$  and determines whether to accept or reject the set of parameters by using the Metropolis-Hastings algorithm.

## RESULTS AND DISCUSSION

We report mean parameter values and boundaries of the symmetric 68 and 95% ( $1\sigma$  and  $2\sigma$  confidence intervals (C.L.) for all the models in Table 2, respectively. Before further analysis, we first explained the value of  $\chi^2$ . The BAO-only data obtain  $\chi^2 = 2.272$  in the  $\Lambda$ CDM model, and the Planck/BAO data gave  $\chi^2 = 1.986$ . Considering the numbers of the BAO and CMB/BAO data are both 13, while the  $\chi^2$  is small. And, limited improvement of  $\chi^2$  is given out after adding the  $\Omega_b h^2$  prior to extending of the  $\Lambda$ CDM

model. Lazkoz et al. (2013) concluded this phenomenon is due to parricidal overlap in both redshift and sky coverage for WiggleZ and BOSS. As we neglect interdependence between constraints from different surveys, our overlap dataset also have the same small  $\chi^2$ .

Basically, all the data are effective to give out an accelerating universe as shown in Figure 1. The derived decelerating parameter  $q(z) = -aa''/a'^2$  represents an accelerating universe when  $-1 < q_0 < 0$  and the transition redshift  $z_t$  where  $q(z_t) = 0$  denotes the time when our universe evolved from cosmic deceleration ( $q > 0$ ) to acceleration ( $q < 0$ ).

As a representative, the Planck/BAO data obtain:

$$q_0 = -0.62_{-0.01-0.02}^{+0.04+0.06}, z_t = 0.80_{-0.09-0.11}^{+0.03+0.05} (\Lambda\text{CDM}),$$

$$q_0 = -0.71_{-0.41-0.68}^{+0.33+0.47}, z_t = 0.77_{-0.07-0.13}^{+0.07+0.09} (w\text{CDM}),$$

$$q_0 = -0.62_{-0.06-0.10}^{+0.07+0.12}, z_t = 0.80_{-0.13-0.21}^{+0.13+0.22} (o\Lambda\text{CDM}).$$

Where  $q_0$  and  $z_t$  constraints have nearly identical central value to the most constraining result of BAO + Planck/BAO +  $\Omega_m h^2$  +  $\Omega_b h^2$ , but with larger error. Specially, the  $w$ CDM model gives out the latest transfer redshift and its deceleration parameter is smaller than the ones in the  $\Lambda$ CDM and  $o\Lambda$ CDM models. It is because the fitting value of  $w$  is less than  $-1$  and the universe is accelerating faster.

In general, the  $\Lambda$ CDM give out the tightest constraint while the extended parameter  $w$  and  $\Omega_{k0}$  enlarge the parameter space. Although the chosen procedure is different, it is clear that the BAO+CMB/BAO+ $\Omega_b h^2 + \Omega_m h^2$  data make the main effect of tightening the parameter region. To investigate the CMB and BAO effect separately, we plot the best fit value and parameter contours in Figure 2. The constraining results for all the models are nearly the same between WMAP9/BAO and WMAP9(w)/BAO data for  $\Omega_{m0}$ , and just have a small difference for  $\Omega_{k0}$  and  $w$ . The WMAP9(w)/BAO data could be replaced by the WMAP9/BAO data. Meanwhile, there are obvious shifts

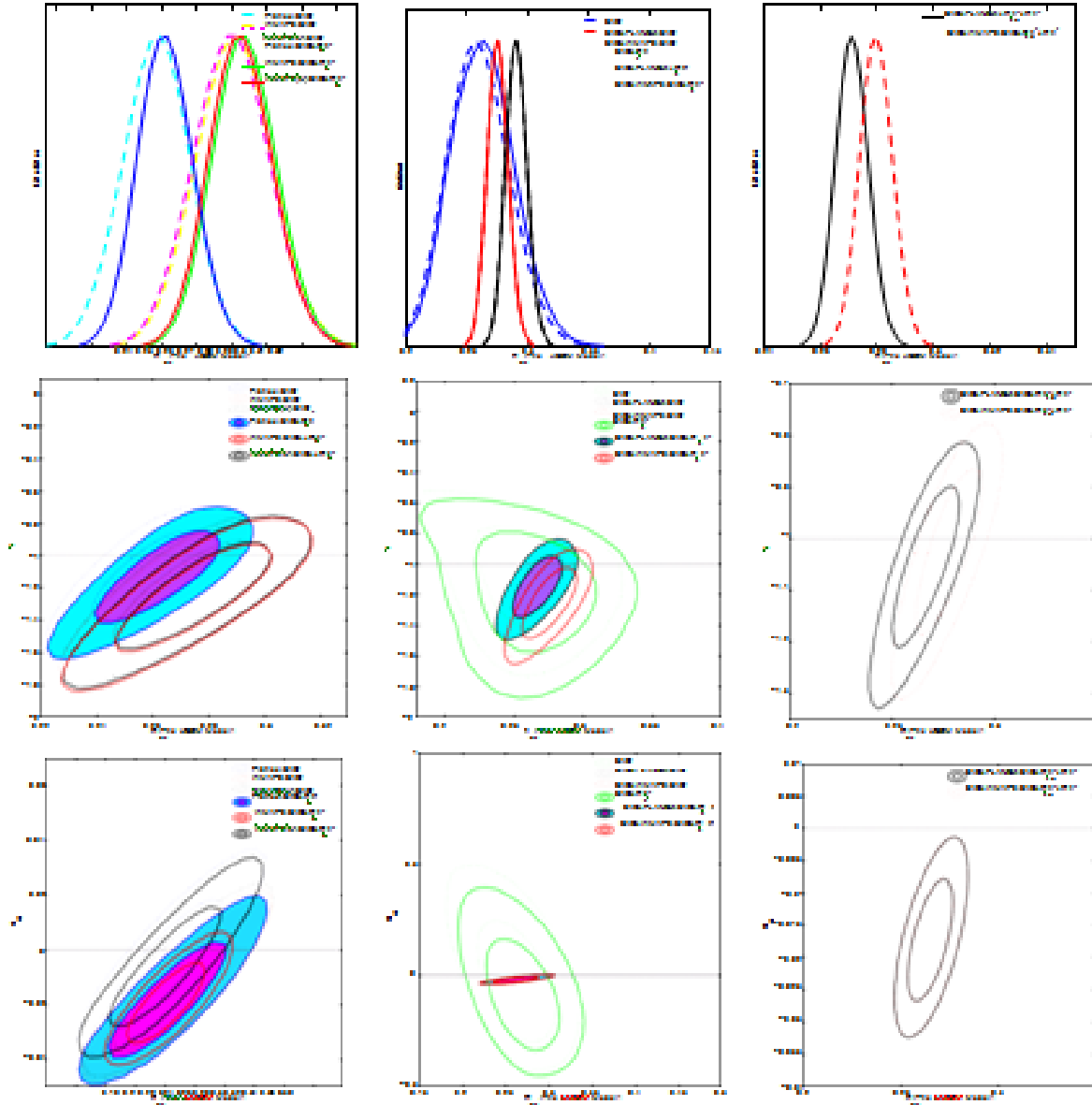


**Figure 2:** The upper three panels are the values of the likelihood of the parameter  $\Omega_{m0}$  for the  $\Lambda$ CDM model. The middle three panels in the transverse direction are the contour plots of  $\Omega_{m0} - w$  for the  $w$ CDM model. The lower three panels are the contour plots of  $\Omega_{m0} - \Omega_{k0}$  for the  $o\Lambda$ CDM model. The left, middle and right three panels are for CMB comparison, BAO comparison and tightest constraint display. The lines  $w = -1$  and  $\Omega_{k0} = 0$  show the fixed values in the  $\Lambda$ CDM model.

between the Planck/BAO and WMAP9/BAO data for the  $\Omega_{m0}$ ,  $\Omega_{k0}$  and  $w$  parameters. The Planck and WMAP9 survey bring different  $l_A$  and  $r_s(z_d)/r_s(z_*)$ , while the WMAP9/BAO and WMAP9( $w$ )/BAO<sup>0.035</sup> have the same  $r_s(z_d)/r_s(z_*)$ . The result of Planck/BAO, WMAP9/BAO and WMAP9( $w$ )/BAO are expected because the error for  $r_s(z_d)/r_s(z_*)$  is 1% while that for  $l_A$  is 0.02%. The different results between Planck/BAO and WMAP9/BAO shown through the recombination history are not related to the CMB/BAO data directly, it determined the value and error of the CMB/BAO data.

### The $\Omega_{m0}$ parameter

For the  $\Lambda$ CDM model, the BAO+Planck/BAO+ $\Omega_b h^2 + \Omega_m h^2$  data give out  $\Omega_{m0} = 0.271^{+0.011+0.016}_{-0.010-0.015}$  which has an obvious tension with the Planck+WP+highL+BAO result where  $\Omega_{m0} = 0.308 \pm 0.010$  (68%). Our result has a tension with the SNLS data which shows  $\Omega_{m0} = 0.227^{+0.042}$  (68%), such is the Planck result. The tension between Planck and SNLS could be regarded as the systematics in SNLS SNe IA data and as such could be also used to explain our results. Our results is consistent with the Union2.1 data where  $\Omega_{m0} =$

$0.295^{+0.043}$  (68%) and the JLA data where  $\Omega_{m0} = 0.295 \pm 0.034$  (68%)<sup>3</sup>. The tension of  $\Omega_{m0}$  between the Planck data and our results could be alleviated by extending parameters.

The BAO+Planck/BAO+ $\Omega_b h^2 + \Omega_m h^2$  data give out  $\Omega_{m0} = 0.267^{+0.022+0.031}$  for the  $w$ CDM model. Anyway, the final solution to the tension problem should consider the recombination history because the best fit of  $\Omega_{m0}$  of the BAO+WMAP9/BAO+ $\Omega_b h^2 + \Omega_m h^2$  data is shifted for the  $\Lambda$ CDM and  $w$ CDM models as compared to the BAO+Planck/BAO+ $\Omega_b h^2 + \Omega_m h^2$  data.

### The extended parameter $w$ and $\Omega_{k0}$

Both the CMB/BAO-only and BAO-only data give a very weak constrain on  $\Omega_{k0}$  and  $w$ . Luckily, they yield different degeneracy directions for  $\Omega_{m0} - w$  and  $\Omega_{m0} - \Omega_{k0}$  which are slightly positive degenerated in CMB/BAO which means when  $\Omega_{m0}$  increases,  $w$  increases, but negatively degenerated in BAO means when  $\Omega_{m0}$  increases,  $w$  decreases. The BAO+CMB/BAO data give out a much tighter constraints and favor the CMB/BAO direction slightly for both  $\Omega_{k0}$  and  $w$  as shown in Figure 2. Due to the two-dimensional geometric degeneracy, the Planck+WP+BAO data alone constrain the range of the EOS of dark energy as  $w = -1.13^{+0.24}$  (95%). Similarly, our results of BAO+Planck/BAO+ $\Omega_b h^2 + \Omega_m h^2$  show  $w = -1.042^{+0.196+0.267}$ . Comparing the contours and the  $w = -1$  line in Figure 2, our results slightly favor phantom where  $w < -1$ .

The CMB curvature power spectrum measurements suffer from a well-known “geometrical degeneracy” which is broken through the integrated Sachs-Wolfe (ISW) effect on large angular scales and gravitational lensing of the CMB spectrum and with the addition of probes of late time physics, the geometrical degeneracy can be broken. Our CMB/BAO results show it could constrain the curvature effectively which favor a small negative  $\Omega_{k0}$  with the precision of  $10^{-2}$ . The accuracy of the BAO+Planck/BAO+ $\Omega_b h^2 + \Omega_m h^2$  results which show  $\Omega_{k0} = -0.017^{+0.020}$  (95%) is close to the Planck+Lensing+WP+highL result where  $\Omega_{k0} = -0.01$  (95%), but has larger error than the Planck+Lensing+WP+highL+BAO results where  $\Omega_{k0} = -0.001$  (95%).

### The $H_0$ parameter

<sup>3</sup> JLA is obtained from the joint analysis of the SDSS-II and SNLS (Supernova Legacy Survey three year sample) collaborations.

Adding the  $\Omega_b h^2$  (or  $\Omega_m h^2$ ) prior only affect the  $\Omega_{m0}$  and  $\Omega_{k0}$  parameters slightly as Figure 2 shows, but it affects the  $H_0$  parameter heavily as shown in Figure 3. To do effective containing, we set a range of  $H_0$ :  $30 \text{ km s}^{-1} \text{ Mpc}^{-1} \leq H_0 \leq 90 \text{ km s}^{-1} \text{ Mpc}^{-1}$ . Table 2 shows the BAO data only gives a lower bound to the  $H_0$  which is around 40. After plus the  $\Omega_b h^2$  prior, the accuracy of  $H_0$  is increased to 5% as shown in Figure 3. And, the constraint tendency between  $H_0$  and  $H_0 r_s$  and  $H_0$  are the same which indicates the  $H_0$  constraint is brought by the  $\Omega_b h^2$  prior. On the other hand, the CMB/BAO data could not constrain the  $H_0$  before adding the  $\Omega_m h^2$  prior. The Planck/BAO+ $\Omega_m h^2$  gives out the  $66.6^{+1.8+2.9} \text{ km s}^{-1} \text{ Mpc}^{-1}$  which is tighter than the BAO+ $\Omega_b h^2$  data. As for the degeneracy between  $\Omega_{m0} - H_0$ , Figure 3 shows BAO and CMB/BAO related data yield different degeneracy directions. They are slightly positive corrected in BAO related data, but negatively related in CMB/BAO and the CMB/BAO+BAO data favor the CMB/BAO direction.

The Planck+WP+highL results get  $H_0 = (67.3 \pm 1.2) \text{ km s}^{-1} \text{ Mpc}^{-1}$  (68%), while the local distance ladder measurements obtain  $H_0 = (73.8 \pm 2.4) \text{ km s}^{-1} \text{ Mpc}^{-1}$  measured using Cepheid variable stars and low-redshift type IA SNe observed with the Hubble Space Telescope (HST) by Riess et al. (2011) and Freedman et al. (2012). Our BAO+Planck/BAO+ $\Omega_b h^2 + \Omega_m h^2$  results show  $66.7^{+1.4+2.1} \text{ km s}^{-1} \text{ Mpc}^{-1}$  which does not have tension with the Planck results, but has mild tensions with local distance ladder measurement of  $H_0$  in the context of  $\Lambda$ CDM model. The tension comes either from some sources of unknown systematic errors in some astrophysical measurements or the wrong  $\Lambda$ CDM model applied in fitting the data. After adding the parameter  $\Omega_{k0}$  and  $w$ , this tension is alleviated slightly in our results where the parameter  $\Omega_{k0}$  and  $w$  enlarge the  $H_0$  range.

### CONCLUSION

Here, we obtain CMB/BAO samples with 13 data in the range of  $0.106 \leq z \leq 2.34$  and focus on parameter constraints and model tests. Basically, the CMB/BAO data give out a tighter constraint as compared to the BAO data though its error increased. The degeneracies of  $\Omega_{m0} - w$  and  $\Omega_{m0} - \Omega_{k0}$  are positive for the CMB/BAO data while it is negative for the BAO distance ratio data.

Fitting the theoretic models to the BAO+Planck/BAO+ $\Omega_b h^2 + \Omega_m h^2$  data, we get constraints on  $\Lambda$ CDM model as  $\Omega_{m0} = 0.271^{+0.011+0.016}$  and  $H_0 = 66.7^{+1.4+2.1} \text{ km s}^{-1} \text{ Mpc}^{-1}$ ;

$$-0.010-0.015$$

$$-1.4-2.1$$

constraints on the  $w$ CDM model as  $\Omega_{m0} = 0.267^{+0.022+0.031}$ ,  $w = -1.042^{+0.196+0.267}$  and  $H_0 = 66.7^{+1.4+2.1} \text{ km s}^{-1} \text{ Mpc}^{-1}$ ;

and constraints on the  $\Lambda$ CDM model from the Planck/CMB as  $\Omega_{m0} = 0.265^{+0.017+0.024}$ ,  $\Omega_{k0} = -0.017^{+0.014+0.020}$  and  $H_0 = 67.2^{+1.9+2.7} \text{ km s}^{-1} \text{ Mpc}^{-1}$ ;

$$-3.0-4.2$$

$$-0.016-0.022$$

$$-0.013-0.018$$

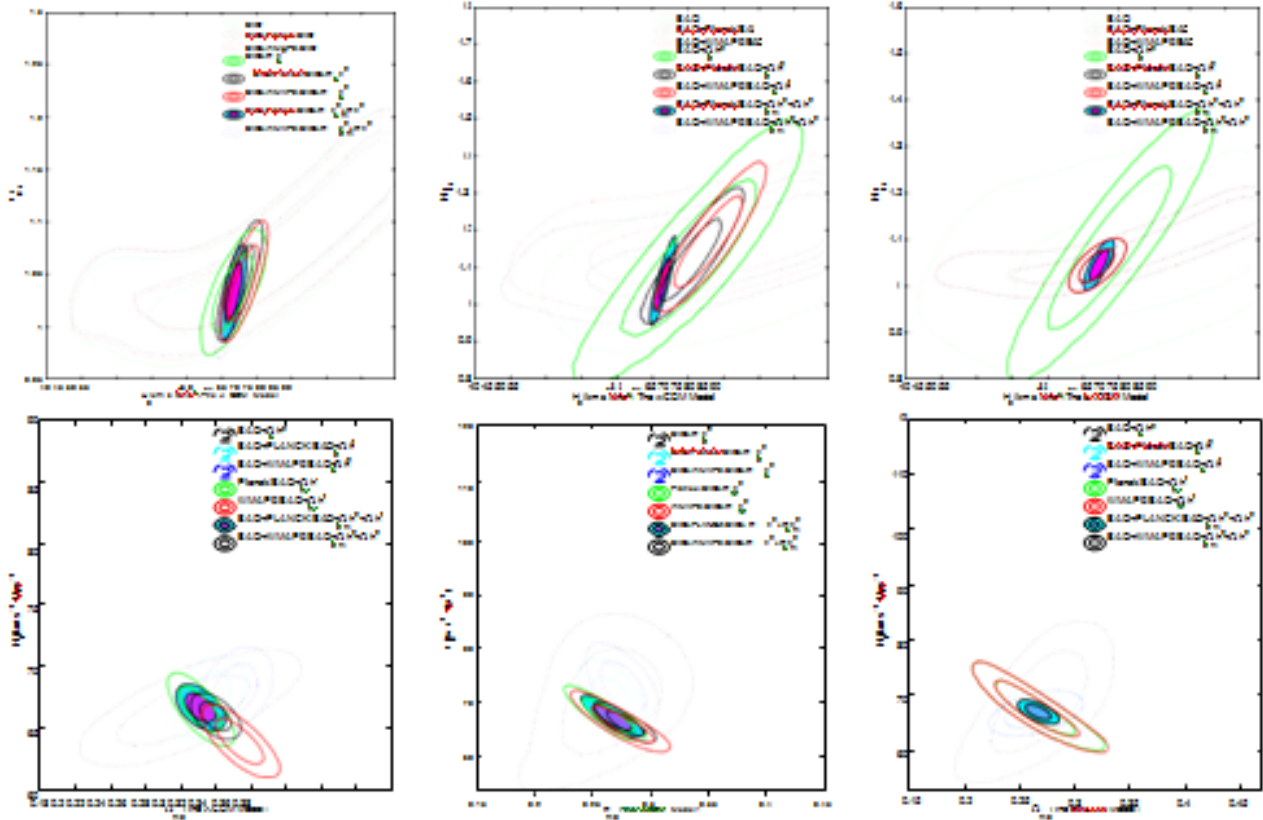


**Figure 3:** The upper and lower three panels are the contour plots of  $H_{0r_s} - H_0$  and  $H_0 - \Omega_{m0}$  separately for the  $\Lambda$ CDM,  $w$ CDM and  $o\Lambda$ CDM models.

### Mpc-1.

All our data about  $\Omega_{m0}$  have tension with the Planck result, but consistent with the SNe data. As for  $H_0$ , our result is consistent with the Planck data, but has tension with the local measurements. And, our results slightly favor phantom dark energy where  $w < -1$  and a negative  $\Omega_{k0}$ .

### ACKNOWLEDGEMENTS

The author wish to appreciate the effort of Dr. Hui Li and Dr. Zhengxiang Li for their assistance in the course of the work. This work was supported by CQ CSTC under grant No. cstc2015jcyjA00044, CQ MEC under grant No. KJ1500414.

### REFERENCES

Adam R *et al.* [Planck Collaboration], arXiv:1409.5738 [astro-ph.CO].  
 Addison GE, Hinshaw G, Halpern M (2013). Mon. Not. Roy. Astron. Soc. 436: 1674 (2013) [arXiv:1304.6984 [astro-ph.CO].  
 Ade PAR *et al.* (2014). [BICEP2 Collaboration], Phys. Rev. Lett. 112: 241101 [arXiv:1403.3985 [astro-ph.CO].  
 Ade PAR *et al.* [Planck Collaboration], arXiv:1303.5076 [astro-ph.CO].  
 Anderson L *et al.* [BOSS Collaboration], arXiv:1312.4877 [astro-ph.CO].  
 Anderson L, Aubourg E, Bailey S, Bizyaev D, Blanton M, Bolton AS, Aubourg E, Bailey S, Bautista JE, Beutler F, Bhardwaj V, Bizyaev D,

Blanton M, Blomqvist M *et al.*, arXiv:1411.1074 [astro-ph.CO].  
 Bennett CL *et al.* (2013). Astrophys. J. Suppl. 208, 20 [WMAP Collaboration], [arXiv:1212.5225 [astro-ph.CO]].  
 Beutler F *et al.*, Mon. Not. Roy. Astron. Soc. 416, 3017 (2011) [arXiv:1106.3366 [astro-ph.CO]].  
 Blake C *et al.* (2011). Mon. Not. Roy. Astron. Soc. 418: 1707. [arXiv:1108.2635 [astro-ph.CO].  
 Blake C *et al.* (2011). Mon. Not. Roy. Astron. Soc. 415: 2892. arXiv:1105.2862. astro-ph.CO.  
 Brinkmann J, Brownstein JR *et al.* (2013). Mon. Not. Roy. Astron. Soc. 427:4, 3435. arXiv:1203.6594 [astro-ph.CO].  
 Busca NG, Delubac T, Rich J, Bailey S, Font-Ribera A, Kirkby J, Le Goff M, Pieri MM *et al.* (2013). Astron. Astrophys. 552:A96. arXiv:1211.2616 [astro-ph.CO].  
 Cai RG, Guo ZK, Tang B. arXiv:1409.0223 [astro-ph.CO].  
 Cheng C, Huang QG, arXiv:1409.6119 [astro-ph.CO].  
 Delubac T *et al.* [BOSS Collaboration], arXiv:1404.1801 [astro-ph.CO].  
 Eisenstein DJ, Hu W (1997). Astrophys. J. 511:5 [astro-ph/9710252].  
 Freedman WL, Madore BF, Scowcroft V, Burns C, Monson A, Persson SE Jha W, Li W *et al.* (2011). Astrophys. J. 730:119. Erratum-ibid. 732: 129 [arXiv:1103.2976 [astro-ph.CO]].  
 Kazin E (2012). Mon. Not. Roy. Astron. Soc. 427 3: 2132. [arXiv:1202.0090 [astro-ph.CO].  
 Kazin EA *et al.* [SDSS Collaboration], Astrophys. J. 710: 1444. [arXiv:0908.2598 [astro-ph.CO]].  
 Lazkoz R, Alcaniz J, Escamilla-Rivera C, Salzano V, Sendra I (2013). JCAP 1312:005. [arXiv:1311.6817 [astro-ph.CO]].  
 Lewis A, Bridle S (2002). Phys. Rev. D 66, 103511 [astro-ph/0205436].  
 Li Z, Liao K, Wu P, Yu H, Zhu ZH (2013). Phys. Rev. D 88: 2, 023003. arXiv:1306.5932 [gr-qc].  
 Li Z, Wu P, Yu H (2012). Astrophys. J. 744:176. [arXiv:1109.6125 [astro-

ph.CO].

M. Pettini and R. Cooke, (2012). Mon. Not. Roy. Astron. Soc. 425-2477. [arXiv:1205.3785 [astro-ph.CO]].

Manera M, Scoccimarro R, Percival WJ, Samushia L, McBride CK, Ross A, Padmanabhan N, Xu X, Eisenstein DJ, Scalzo R, Cuesta AJ, Mehta KT, Percival WJ, Cole S, Eisenstein DJ, Nichol RC, Peacock JA, Pope AC, Szalay SA (2007). Mon. Not. Roy. Astron. Soc. 381: 1053. arXiv:0705.3323 [astro-ph]].

Riess AG, Macri L, Casertano S, Lampeitl H, Ferguson HC, Filippenko AV, Seibert M, Rigby J (2012). Astrophys. J. 758: 24. [arXiv:1208.3281 [astro-ph.CO]].

Sheth R, White M et al (2012). Mon. Not. Roy. Astron. Soc. 428, no. 2, 1036 (2012) [arXiv:1203.6609 [astro-ph.CO]].

Sollerman J et al (2009). Astrophys. J. arXiv:0908.4276 astro-ph.CO. 703-1374.

Veropalumbo A, Marulli F, Moscardini L, Moresco M., Cimatti A arXiv:1311.5895 [astro-ph.CO].

W. J. Percival *et al.* [SDSS Collaboration], Mon. Not. Roy. Astron. Soc. 401, 2148 (2010) [arXiv:0907.1660 [astro-ph.CO]].

Wang Y, Chuang CH, Mukherjee P (2012). Phys. Rev. D 85, 023517. [arXiv:1109.3172 [astro-ph.CO]].

Wang Y, Wang S (2013). Phys. Rev. D 88, no. 4, 043522. [arXiv:1304.4514 [astro-ph.CO]].

Weinberg DH, Mortonson MJ, Eisenstein DJ, Hirata C, Riess AG, Rozo E (2013). Phys. Rept. 530: 87. [arXiv:1201.2434 [astro-ph.CO]].  
Zhang Y, Gong Y(2013). Mod. Phys. Lett. A 28, no. 35, 1350135.